Modeling of Peptide Hydrolysis by Thermolysin. A Semiempirical and QM/MM Study

Serge Antonczak, Gérald Monard, Manuel F. Ruiz-López, and Jean-Louis Rivail*

Contribution from the Laboratoire de Chimie Théorique, Unité Mixte de Recherche No. 7565, Université Henri Poincaré−Nancy I, BP 239, 54506 Vandœuvre-lès-Nancy Cedex, France

Received May 12, 1998

Abstract: The hydrolysis by thermolysin of formamide, considered as a model of a peptide bond, has been studied with semiempirical and mixed QM/MM methods. The study has been carried out for two catalysts—a molecular complex of a Zn^{2+} ion with two imidazole molecules and a formate ion, modeling the active site of the enzyme, and the whole enzyme—and for two mechanisms involving one and two water molecules. In every case, the first step of the reaction is a nucleophilic attack of the carbon atom by the oxygen of a water molecule or a water dimer. The mechanism involving an ancillary water molecule (water-assisted process) is always favored compared to the process in which a single water molecule reacts. The fact is explained by a better nucleophilicity of the oxygen atom in the water dimer and a less constrained transition state. The zinc atom of the catalytic center acts as a Lewis acid and the ligands as an electron reservoir. The slight differences between the reactions catalyzed by the model complex and by the whole enzyme are explained on the basis of small geometry distortions induced by the amino acids residues surrounding the active center.

I. Introduction

The understanding of the mechanism of enzymatic reactions is of greatest interest. For many years, theoretical studies of such reactions have focused on the active site independently of the rest of the enzyme.[1] Nevertheless, the role of the protein has been shown not to be negligible.[2] The enzymatic activity of zinc metalloprotease is directly related to the presence of Zn^{2+} in its active site.[3] In biology, zinc is the most profuse metal after iron. It carries on its biological activity in association with several proteins, and its catalytic role is very important.[4] The first zinc-containing enzyme discovered was carbonic anhydrase,[5] which permits hydration of carbonic dioxide and bicarbonate deshydration. More than 200 zinc-containing enzymes have been characterized since then. The role of the metal is essentially catalytic,[6,7] but it can also be conformational, giving the protein the ability to keep a stability or a regulating function by activating or inhibiting its catalytic activity. In thermolysin[8] (TLN), an endopeptidase, the role of zinc is essentially catalytic.

Some theoretical works have been devoted to many zinc complexes.[9,10] Recent studies have been devoted to hydration water of Zn(II) ions[11] and to the importance of its ligands in the catalytical activity.[12] Hence, complete studies about zinc, its parametrization, and its role in different catalytic mechanisms have been done.[10,13] Theoretical works have been previously devoted to amide or peptide hydrolysis.[14] It has been shown that, considering nonassisted reactions, stepwise nonprotonated hydrolysis was competitive with the concerted one. In previous works,[15] we have studied in a neutral or protonated way the water-assisted formamide hydrolysis mechanism (i.e., involving two water molecules in the processes), for which stepwise mechanisms are difficult to imagine. Comparisons were made with nonassisted mechanisms (i.e., involving only one water molecule in the processes). We first investigated the whole reaction mechanism at a relatively simple ab initio level.[15a] In that study, the electrostatic role of the solvent was also taken into account. Then, in a following work,[15b] we investigated different methods of computation to assess the accuracy of

* To whom correspondence should be addressed. Tel.: 33-(0)3 83 91 20 50. Fax: 33-(0)3 83 91 25 30. E-mail: rivail@lctn.u-nancy.fr.

(1) Warshel, A. *Computer modeling of Chemical Reactions in Enzymes and Solutions*; J. Wiley and Sons: New York, 1991.

(2) Warshel, A.; Lewitt, M. *J. Mol. Biol.* **1976**, *103*, 227.

(3) (a) Lipscomb, W. N.; Sträter, N. *Chem. Rev.* **1996**, *96*, 2375. (b) Vallé, B. L.; Auld, D. S. *Faraday Discuss.* **1992**, *93*, 47.

(4) Vallé, B. L.; Wacker, W. E. C. In *The Proteins*; Neurath, H., Ed.; Academic: New York, 1970; p 5.

(5) Keilin, D.; Mann, T. *Biochem. J.* **1940**, *34*, 33.

(6) Vallé, B. L. In *Zinc Enzymes*; Bertini, I., Luchinat, C., Maret, W., Zeppezauer, M., Eds.; Birkhauser: Boston, 1986; p 5.

(7) Formicka-Kozlowska, G.; Maret, W.; Zeppezauer, M. In *Zinc Enzymes*; Bertini, I., Luchinat, C., Maret, W., Zeppezauer, M. Eds.; Birkhauser: Boston, 1986; p 579.

(8) Fersht, A. In *Enzyme Structure and Mechanism*; W. H. Freeman and Co.: New York, 1985.

(9) (a) Pullman, A.; Demoulin, D. *Int. J. Quantum Chem.* **1978**, *14*, 779. (b) Bertran, J. *Computational Advances in Organic Chemistry;* NATO ASI Series 330; Kluwer: Dordrecht, 1989. (c) Tossel, J. A. *Chem. Phys. Lett.* **1990**, *169*, 145.

(10) Jacob, O. Thése de l'Université Louis Pasteur de Strasbourg I, 1990.

(11) (a) Hartmann, M.; Clark, T.; van Eldik, R. *J. Am. Chem. Soc.* **1997**, *119*, 7843. (b) Hartmann, M.; Clark, T.; van Eldik, R. *J. Mol. Model.* **1996**, *2*, 354.

(12) (a) Cini, R.; Musaev, D. G.; Marzilli, L. G.; Morokuma, K. *J. Mol. Struct. THEOCHEM* **1997**, *392*, 55. (b) Gresh, N.; Stevens, W. J. *J. Comput. Chem.* **1995**, *7*, 843.

(13) Hartmann, M.; Clark, T.; van Eldik, R. *J. Mol. Model.* **1996**, *2*, 358.

(14) (a) Oie, T.; Loew, G. H.; Burt, S. K.; Binkley, J. S.; MacElroy, R. D. *J. Am. Chem. Soc.* **1982**, *104*, 6169. (b) Krug, J. P.; Popelier, P. L. A.; Bader, R. F. W. *J. Phys. Chem.* **1992**, *96*, 7604. (c) Jensen, J. H.; Baldridge, K. K.; Gordon, M. S. *J. Phys. Chem.* **1992**, *96*, 8340. (d) Dobbs, K. D.; Dixon, D. A. *J. Phys. Chem.* **1996**, *100*, 3965. (e) Cho, S. J.; Cui, C.; Lee, J. Y.; Park, J. K.; Suh, S. B.; Park, J.; Kim, B. H.; Kim, K. S. *J. Org. Chem.* **1997**, *62*, 4068. (f) Hori, K.; Kamimura, A.; Ando, K.; Mizumura, M.; Ihara, Y. *Tetrahedron* **1997**, *53*, 4317.

(15) (a) Antonczak, S.; Ruiz-López, M. F.; Rivail J.-L. *J. Am. Chem. Soc.* **1994**, *116*, 3912. (b) Antonczak, S.; Ruiz-López, M. F.; Rivail J.-L. *J. Mol. Model* **1997**, *3*, 434.

S0002-7863(98)01650-3 CCC: $15.00
Published on Web 08/11/1998

semiempirical computations. The results obtained in this study predict a relatively good agreement between ab initio, DFT, and semiempirical geometries, but the semiempirical activation energies remain overestimated.

There exist several quantum studies devoted to enzymatic mechanisms[16] but only a few involving zinc enzymes, such as carboxypeptidase A[13,17] or alcohol dehydrogenase.[18] In these proteins, zinc ligands are histidine or glutamate amino acids, as found in thermolysin or several other enzymes. Interactions between these amino acids and the metal and their influence on the structures and functions of a precise protein have also been studied.[12a,18b,19] Pardo et al.[20] examined some models of proton transfer in biological systems. Merz et al.[21] were the first to demonstrate that, using semiempirical methods such as AM1, it is possible to tackle the study of enzyme models. Good accordance between AM1 calculations and experimental results or ab initio computations has been shown by Merz and Dewar[22] In an ab initio study devoted to the carbonic anhydrase mechanism, Jacob et al.[23] made comparisons between their results and these obtained by Merz and Dewar and noted that AM1 gives relatively good results for the transition states structures, but they have already pointed out that activation barriers are overestimated.

An accurate theoretical description of the active site of an enzyme such as thermolysin requires taking into account the metal ion and its environment. This environment plays an important role in the catalytic properties of the system, but its definition is not simple, so several residues may be involved in the course of the reaction. In particular, it is assumed that the ligands of Zn^{2+} play an important role, for example, in delocalizing the charges along the reaction path. Describing a reaction requires the use of quantum mechanics, but a large number of atoms in a system described quantically, by ab initio, DFT, or even semiempirical methods, would lead to prohibitively time-consuming computations. Such studies are now feasible thanks to several simplifications introduced to represent the largest part of the system, which need not be treated quantum mechanically.[1,2] In particular, mixed methods have developed recently. In these models, the fraction of the enzyme which is assumed to play the major role in the reaction is treated by quantum mechanics, while the rest of the system is described by a classical force field. These methods are denoted by QM/MM.

Most of such methods are limited to the semiempirical level,[24] although hybrid density functional and ab initio methods have been developed as well.[25] Enzymatic reactions are a very appealing field for QM/MM methods, and, indeed, several studies have already been published,[26] but, to our knowledge, only a few metalloenzymes have been considered at this level of modeling. In addition, contrary to the standard methods, which use an artificial link atom to treat the quantum subsystem as a model molecule, this study is an attempt to use the local self-consistent field method[27,28] (LSCF), which treats explicitly the bond separating the quantum part from the classical one. This separation is very important, since it can strongly influence the results of the quantum computation.

In the present work, we focused our attention on the hydrolysis by thermolysin of formamide, considered as a model peptide. This study will be carried out progressively. We first start with a quantum study on a small system, where only the metal, some model ligands, and the substrate are considered. Semiempirical optimizations followed by DFT single-point energy calculations allow us to assess the role of the ligands in the catalytic reaction. The influence of the whole enzyme is then taken into account using the QM/MM LSCF method mentioned above. In a future work,[29] the hydrolysis of a whole peptide by thermolysin and the role of the most important amino acids[30,31] will be considered and discussed.

II. Methods of Computation

Semiempirical computations are performed using the GEOMOS[32] program at the NDDO level with AM1 parametrization.[33] QM/MM calculations make use of the LSCF[27,28] formalism, which describes the separation between the quantum subsystem and the classical one by frozen, strictly localized bond orbitals (SLBO). At the NDDO level, the participation of the quantum frontier atom to the SLBO reduces to a hybrid orbital (HO)[27b] and is fully determined by the s/p ratio (a_s)

(16) (a) Pitarch, J.; Ruiz-López, M. F.; Pascual-Ahuir, J.-L.; Silla, E.; Tuñón, I. *J. Phys. Chem. B* **1997**, *101*, 3581. (b) Frau, J.; Donoso, J.; Muñoz, F.; García Blanco, F. *J. Comput. Chem.* **1991**, *13*, 681 (see also references therein). (c) Rivail, J.-L.; Loos, M.; Théry, V. In *Trends in Ecological Physical Chemistry*; Bonati, L., Cosentino, U., Lasagni, M., Moro, G., Pitea, D., Schiraldi, A., Eds.; Elsevier: Amsterdam, 1993; pp 17−26. (d) Beveridge, A. J.; Heywood, G. C. *J. Mol. Struct. THEOCHEM* **1994**, *306*, 235. (e) Beveridge, A. J.; Heywood, G. C. *Biochemistry* **1993**, *32*, 3325. (f) Lee, H.; Darden, T. A.; Pedersen, L. G. *J. Am. Chem. Soc.* **1996**, *118*, 3946.

(17) (a) Alex, A.; Clark, T. *J. Comput. Chem.* **1992**, *13*, 704. (b) Sakurai, M.; Furuki, T.; Inoue, Y. *J. Phys. Chem.* **1995**, *99*, 17789. (c) Alvarez-Santos, S.; González-Lafont, A.; Lluch, J. M.; Oliva, B.; Avilés, F. X. *New J. Chem.* **1996**, *20*, 979. (d) Andrés, J.; Moliner, V.; Safont, V. S.; Domingo, L. R.; Picher, M. T. *J. Org. Chem.* **1996**, *61*, 7777.

(18) (a) Riter von Onciul, A.; Clark, T. *J. Comput. Chem.* **1993**, *14*, 392. (b) Vanhommerig, S. A. M.; Meier, R. J.; Sluyterman, L. A.Æ.; Meijer, E. M. *J. Mol. Struct. THEOCHEM* **1996**, *364*, 33.

(19) Christianson, D. W.; Alexander, R. S. *J. Am. Chem. Soc.* **1989**, *111*, 6412.

(20) Pardo, L.; Mazurek, A. P.; Osman, R. *Int. J. Quantum Chem.* **1990**, *37*, 701.

(21) Merz, K. M., Jr.; Hoffmann, R.; Dewar, M. J. S. *J. Am. Chem. Soc.* **1989**, *111*, 5636.

(22) Merz, K. M., Jr.; Dewar, M. J. S. *Organometallics* **1988**, *7*, 522.

(23) Jacob, O.; Cardenas, R.; Tapia, O. *J. Am. Chem. Soc.* **1990**, *112*, 8692.

(24) For reviews, see: (a) Gao, J. In *Reviews in Computational Chemistry*, Lipkowitz K. B., Boyd D. B., Eds.; VCH Publishers: New York, 1996; Vol. 7. (b) Åqvist, J.; Warshel, A. *Chem. Rev.* **1993**, *93*, 2523. (c) Ruiz-López, M. F.; Rivail, J.-L. In *Encyclopedia of Computational Chemistry*; Schleyer, P. v. R., Ed.; Wiley & Sons: New York, in press.

(25) (a) Tuñón, I.; Martins-Costa, M. T. C.; Millot, C.; Ruiz-López, M. F. *J. Mol. Model* **1995**, *1*, 196. (b) Tuñon, I.; Martins-Costa, M. T. C.; Millot, C.; Ruiz-López, M. F. *J. Chem. Phys.* **1997**, *106*, 3633. (c) Strnad, M.; Martins-Costa, M. T. C.; Millot, C.; Tuñón, I.; Ruiz-López, M. F.; Rivail, J.-L. *J. Chem. Phys.* **1997**, *106*, 3643.

(26) (a) Cunningham, M. A.; Ho, L. L.; Nguyen, D. T.; Gillilian R. E.; Bash, P. A. *Biochemistry* **1997**, *36*, 4800. (b) Ranganathan, S.; Gready, J. E. *J. Phys. Chem. B.* **1997**, *101*, 5614. (c) Liu, H.; Müller-Plathe, F.; van Gunsteren, W. F. *J. Mol. Biol.* **1996**, *261*, 454. (d) Lyne, P. D.; Mulholland, A. D.; Richards W. G. *J. Am. Chem. Soc.* **1995**, *117*, 11345. (e) Arad, D.; Langridge R.; Kollman, P. A. *J. Am. Chem. Soc.* **1990**, *112*, 491.

(27) (a) Théry, V.; Rinaldi, D.; Rivail, J.-L.; Maigret, B.; Ferenczy, G. *J. Comput. Chem.* **1994**, *15*, 269. (b) Monard, G.; Loos, M.; Théry, V.; Baka, K.; Rivail, J.-L. *Int. J. Quantum Chem.* **1996**, *58*, 153.

(28) (a) Assfeld, X.; Rivail, J.-L. *Chem. Phys. Lett.* **1996**, *263*, 100. (b) Assfeld, X.; Ferré, N.; Rivail, J.-L. In *Methods and Applications of Hybrid Quantum Mechanical and Molecular Mechanical Methods*; Gao, J., Ed.; ACS Symposium Series; American Chemical Society: Washington, DC, in press.

(29) Antonczak, S.; Monard, G.; Ruiz-López, M. F.; Rivail J.-L. Work in progress.

(30) (a) Beaumont, A.; O'Donohue, M. J.; Roques, B. P. *J. Biol. Chem.* **1995**, *270*, 16803. (b) Marie-Claire, C.; Ruffet, E.; Antonczak, S.; Beaumont, A.; O'Donohue, M. J.; Roques, B. P.; Fournié-Zaluski, M. C. *Biochemistry* **1997**, *36*, 13938.

(31) (a) Matthews, B. W. *Acc. Chem. Res.* **1988**, *21*, 333. (b) Mock, W. L.; Aksamawati, M. *Biochem. J.* **1994**, *302*, 57. (c) Mock, W. L.; Stanford, D. J. *Biochemistry* **1996**, *35*, 7369.

(32) Rinaldi, D.; Hoggan, P. E.; Cartier, A. GEOMOS: Semiempirical SCF System for Dealing with Solvent Effects and Solid Surface Adsorption (QCPE 584a). *QCPE Bull.* **1989**, 128.

(33) (a) Stewart, J. J. P. *J. Comput. Chem.* **1989**, *10*, 221 (for O, C, H, and N atoms). (b) Merz, K. M., Jr.; Dewar, M. J. S. *Organometallics* **1988**, *7*, 522 (for Zn atom).

and its coefficient in the SLBO or, equivalently, the density matrix element P_{ll} for the element of the second row of the periodic table. These parameters are extracted from calculations on model systems. If X denotes an amino acid which will share a SLBO with the classical part, then a full AM1 computation is performed on a Gly-X-Gly tripeptide. A localization procedure is applied to the optimized structure, and the renormalized SLBO is transferred into the whole protein. The computation of the molecular orbitals of the quantum fragment, at the NDDO level of approximation, requires only the replacement of the atomic orbitals of each frontier atom by linear combinations orthogonal to the frozen hybrid one. This requires only a simple linear transformations of the Hartree−Fock equations[27a] and is performed in the GEOMOP[34] program. In the present work, the classical environment is kept fixed during the calculations. It interacts with the quantum subsystem only by means of electrostatic and van der Waals interactions.

The transition states have been located using Schlegel's algorithm[35] and characterized by the Hessian matrix, verifying that they present only one negative eigenvalue, corresponding to an imaginary frequency. Reaction intermediates have been shown to be related to the TS by following the transition vector on both sides (IRC formalism[36]) and then fully optimized.

DFT single-point calculations have been carried out, using the optimized AM1 structures in order to obtain better values of the energy barriers. They have been performed using the conventional procedures available in the Gaussian92/DFT[37] package. BLYP is the chosen potential. It employs Becke exchange functional[38] and Lee−Yang−Parr correlation functional.[39] Becke functional includes gradient-corrected Slater exchange. Lee−Yang−Parr functional includes both local and gradient corrections. In a previous work,[15b] it has been shown that BLYP results agree quite well with MP2 and AM1 calculations for our type of reaction, except in some special cases. DZVP2[40] (63321/5211*/41+), the Gaussian-type basis set implemented in the DeMon[41] program, has been chosen for these calculations. Hereafter, the following notations will be used: BLYP//AM1 means that a single-point calculation at the BLYP/DZVP2 level has been performed using the optimized geometry at AM1 level.

All our computations are based on a crystallographic structure of thermolysin,[42] found in the Protein Data Bank, including the water molecules present in the crystal. The minimization procedures have been performed using the DISCOVER program developed by BIOSYM.[43] We have used the AMBER[44] force field in which the parameters for the zinc atom,[10] obtained from ab initio calculations, have been included. Minimizations have been performed using either steepest descent or conjugate gradients methods without any constraints.

III. Hydrolysis of Formamide by a Model System of the Active Site

In the wild-type thermolysin, the ligands of the Zn^{2+} center are two histidines (His142 and His146), one glutamate residue (Glu166), and a solvation water molecule (see Chart 1). In the hydrolysis mechanism, the substrate replaces the water molecule as the fourth ligand on the metal center. The study of such a simple complex, considered as a catalyst, separated from the rest of the enzyme is expected to give preliminary information on the strength of the enzyme. In particular, the electronic properties of the ligands are expected to play an important role in the Lewis acidity of the zinc metal center and, consequently, in the activation of the substrate. To study such a catalyst, a simple complex where histidine and glutamate ligands were replaced by imidazole and formate groups, respectively, has been considered (Figure 1). It has been shown[12a] that replacing histidines by NH_3 is not satisfactory and that using imidazole groups as models is acceptable. The size of this system remains relatively limited and thus can be studied by means of quantum methods. Following previous works on amide hydrolysis,[15] we have considered both a water-assisted mechanism (bifunctional catalysis) and a nonassisted mechanism. In the former case, an ancillary water molecule which enters the reaction coordinate has to be added to the system.

In the system chosen for this study, almost 25 atoms are present around the metal. Thus, ab initio calculations being already time-consuming, geometry optimizations have been carried out at the AM1 semiempirical level, followed by single-point energy calculations at the DF level using the AM1-optimized structures. Previous work[15b] has shown that, for these systems, this scheme of calculation is acceptable, especially in the case of catalyzed reactions. Here, the structure of the fully optimized active site model remains close to the crystallographic geometry (see Table 1). Because of the necessity to take into account the relaxation of the system when considering the

Chart 1

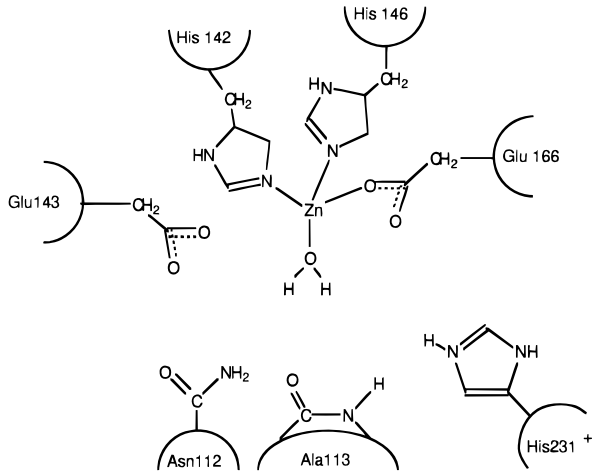

Table 1. Geometrical Parameters Corresponding to the Complex and to the Transition States[a]

	FoC	TS1C	TS2C
ZnO_1	2.163	2.124	2.098
C_1O_1	1.280	1.323	1.342
C_1N_1	1.343	1.493	1.474
C_1O_1'		1.506	1.488
$O_1'H_1'$		1.278	1.388
N_1H_1'		1.404	
$H_1'O_2'$			1.102
$O_2'H_2'$			1.034
N_1H_2'			1.765
$H_1'O_1'C_1N_1$		−1.11	13.02
$O_2'H_1'O_1'C_1$			15.04
$H_2'O_2'H_1'O_1'$			−25.08

[a] Bond lengths in angstroms and angles in degrees. See text and Figures 1 and 2 for notations.

(34) Rinaldi, D.; Hoggan, P. E.; Cartier, A.; Baka, K.; Monard, G.; Loos, M.; Mokrane, A.; Dillet, V.; Thery, V. *GEOMOP*, to be published.
(35) Schlegel, H. B. *J. Comput. Chem.* **1982**, *3*, 214.
(36) (a) Gonzales, C.; Schlegel, H. B. *J. Phys. Chem.* **1990**, *94*, 5523. (b) Beapark, M. J.; Robb, M. A.; Schlegel, H. B. *Chem. Phys. Lett.* **1994**, *223*, 269.
(37) Frish, M. J.; Trucks, G. W.; Head-Gordon, M.; Gill, P. M. W.; Wong, M. W.; Foresman, J. B.; Johnson, B. G.; Schlegel, H. B.; Robb, M. A.; Reprogle, E. S.; Gomperts, R.; Andres, J. L.; Raghavachari, K.; Binkley, J. S.; Gonzales, C.; Martin, R. L.; Fox, D. J.; Defrees, D. J.; Baker, J.; Stewart, J. J. P.; Pople, J. A. *Gaussian 92/DFT*; Carnegie-Mellon Quantum Chemistry Publishing Unit: Pittsburgh, PA, 1992.
(38) Becke, A. D. *J. Chem. Phys.* **1988**, *88*, 2547.
(39) Lee, C.; Yang, W.; Parr, R. G. *Phys. Rev. B* **1988**, *37*, 786.
(40) Godbout, N.; Salahub, D. R.; Andzelm, J.; Wimmer, E. *Can. J. Chem.* **1992**, 560.
(41) St. Amand, A.; Salahub, D. R. *Chem. Phys. Lett.* **1990**, *169*, 387.
(42) Holmes, M. A.; Matthews, B. W. *J. Mol. Biol.* **1982**, *160*, 623.
(43) Biosym Technologies, Inc., 9685 Scanton Rd., San Diego, CA 92121-4778.
(44) Weiner, S. J.; Kollman, P. A.; Nguyen, D. T.; Case, D. A. *J. Comput. Chem.* **1986**, *7*, 230.

Table 2. Mulliken Net Atomic Charges Corresponding to the Complexes and the Transition States Computed with the Model of Active Site at AM1 Level[a]

	H_2O model[b]	FoC	TS1C	TS2C
		Catalytic Site		
imidazole 1	+0.340	+0.325	+0.316	+0.307
imidazole 2	+0.328	+0.311	+0.307	+0.300
formate	−0.550	−0.591	−0.611	−0.624
Zn	+0.735	+0.711	+0.704	+0.700
total	+0.853	+0.756	+0.716	+0.683
		Reactive Part		
H_2O in thermolysin				
O	−0.408			
H	+0.282			
H	+0.273			
formamide				
O_1		−0.396	−0.547	−0.578
C_1		+0.293	+0.273	+0.279
N_1		−0.357	−0.360	−0.444
subtotal		+0.244	−0.028	−0.231
H_2O in the TS				
O_1'			−0.331	−0.429
H_1'			+0.372	+0.355
O_2'				−0.255
H_2'				+0.332
subtotal			+0.312	+0.547
total	+0.147	+0.244	+0.284	+0.316

[a] See text and Figures 1 and 2 for notations. [b] Optimized H_2O model of active-site complex.

introduction of the formamide molecule, the complex described hereafter has also been totally optimized.

We used the following notation: the formamide−catalyst complex is noted FoC, while TS1C and TS2C denote the transition states of the nonassisted and water-assisted mechanisms, respectively. Geometrical parameters corresponding to these structures are summarized in Table 1. In Table 2 are compiled the Mulliken net atomic charges for the AM1-optimized structures.

A. Model System of the Active Site. The model of the active site is limited to a complex of two imidazoles, one formate ligand, and a water molecule. The Lewis acid properties of the zinc atom are manifested by the charge of the water molecule, +0.147 e (Table 2). A similar study,[17b,45] carried on a model of carbonic anhydrase in which the ligands of Zn^{2+} are three imidazole and one water molecule, gave for the charge of the water molecule +0.167 e. The difference is easily understood if one considers the better electron-donating properties of the formate ligand compared to imidazole. The charge of the zinc atom is less modified: +0.735 e in this study instead of +0.724 e in the case of three imidazoles.

B. Formamide−Catalyst Complex: FoC. In this complex, the formamide is bonded to the metal by its carbonyl group in a same way as a peptide is bonded to the enzyme (see Figure 1 for structures and atom notations). The geometrical parameters of the catalyst are slightly modified by the complexation with formamide. However, though formamide remains planar, comparison with the parameters of the isolated formamide shows a diminution of the C_1N_1 bond (1.343 vs 1.367 Å, respectively) and an increase of the C_1O_1 bond (1.280 vs 1.243 Å, respectively).

The analysis of the electronic population shows a noticeable charge transfer from the formamide molecule, which is left with a total positive charge of 0.244 e, to the complex. This result,

(45) (a) Kvassmann, J.; Larsson, A.; Petterson, G. *Eur. J. Biochem.* **1981**, *114*, 555. (b) Silverman, D. N.; Lindskog, S. *Acc. Chem. Res.* **1988**, *21*, 30.

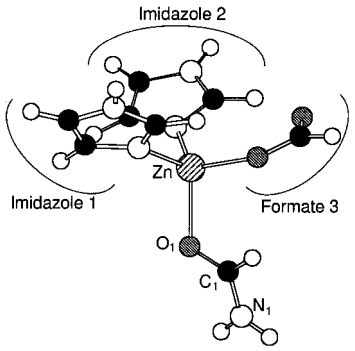

Figure 1. Complex formamide model of active site, denoted FoC. Ligands imidazole 1, imidazole 2, and formate 3 represent respectively the His142, His146, and Glu166 amino acids.

together with the geometric modifications, allows us to interpret the electron flow very easily: the oxygen atom of formamide acts as a very efficient electron donor to the zinc atom. This electron loss induces an important electron donation from carbon to oxygen, increasing the CO bond length and, consequently, a π donation of nitrogen to carbon, explaining the shortening of the C_1-N_1 bond. The overall effect is an increase of the positive charge of the carbon atom (+0.293 vs +0.258 e in the free molecule), which explains the increased electrophilicity of this atom.

Such electronic transfers[17b,d] have already been reported, and the changes in the reactivity of the catalytical systems have been discussed.[12b] In previous work, Vanhommerig et al.[18b] have shown the importance of the total charge of the catalytic system of horse alcohol dehydrogenase, another zinc metalloprotease, through protonation and deprotonation of cysteine amino acids, ligands of the metal center. Depending on whether the zinc ligands are protonated or not, the energy barriers change drastically, and the obtained energy profile is then completely different.

C. Hydrolysis Reaction Study. An attempt to fully optimize the geometry of the system along the reaction path resulted in large geometric modification due to the fact that the system is free of external constrains. These deformations are not compatible with the structure of the active site in the enzyme, in which the host protein forbids large motions of the residues. The optimized structure of the FoC complex being close to the crystallographic geometries in the whole enzyme, we chose to keep it fixed during the hydrolysis process.

Nonassisted Mechanism (TS1C). One single transition state has been located (Figure 2a) between the reactants and the products. With respect to the separate components, i.e., the complexed formamide molecule and the water molecule, the activation energy reaches a rather high value of +49.95 kcal/mol (Table 3). Previous studies on the acid-catalyzed process in a solution[15a] or in a vacuum[15b] told us that the hydrolysis reaction is a concerted process initiated by a nucleophilic attack on the carbon atom of the carbonyl group by the oxygen atom of the water molecule. The same mechanism is observed here, due to the Lewis acid properties of the Zn atom. In the transition state, the C_1O_1' distance between the carbon atom and the oxygen atom of the incoming water molecule (see Figure 2) is 1.506 Å, close to the equilibrium C−O bond length in formic acid (1.37 Å). The N_1H_1' distance is comparatively larger: 1.404 Å. As a consequence of the breaking of the π interactions in the formamide molecule, both the C_1O_1 and C_1N_1 bond lengths increase (+0.043 and +0.150 Å, respectively).

Considering the electron distribution in this system, the most striking feature is that the electron donation to the catalyst by

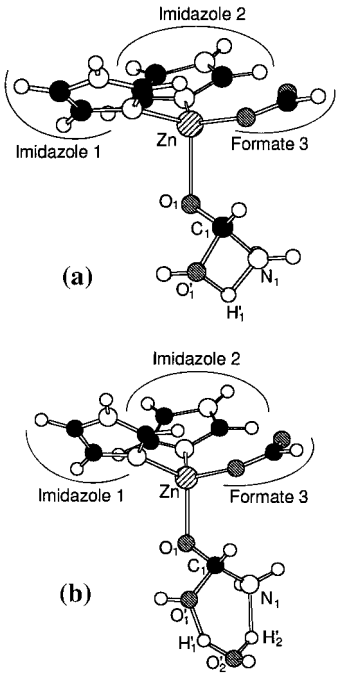

Figure 2. Transition states for the reactions catalyzed by the model of active site, (a) for the nonassisted and (b) for the water-assisted mechanisms (denoted TS1C and TS2C, respectively). See Figure 1 for notations.

Table 3. Relative Energies (in kcal mol^{-1}) Computed at AM1 Level with Respect to the Separate Components[a]

	catalyzed by a model of active site: TS*x*C	catalyzed by thermolysin: TS*x*T	catalyzed by a proton: TS*x*P[b]	neutral: TS*x*N[b]
$x = 1$	49.95	55.48	30.05	58.46
$x = 2$	36.27	38.16	8.16	55.48

[a] Values are given for both the nonassisted (x = 1) and water-assisted mechanisms (x = 2) catalyzed by the model of active site, by the thermolysin, by [H_3O^+], and noncatalyzed. See text for notations. [b] TS1P and TS2P, mechanisms catalyzed by H_3O^+; TS1N and TS2N, neutral mechanisms (see ref 15b).

the reactive species is larger than that in the initial complex. The total Mulliken charge of the formamide + water reactants is now +0.284 e. This electron loss mainly comes from the water molecule, in which the total Mulliken charge is +0.312 e. This charge transfer, which arises through the $O_1'C_1$ interaction, explains the fact that this interatomic distance is shorter in the catalyzed process than in the noncatalyzed one (1.582 Å) but it is longer than in the case of the H_3O^+-catalyzed reaction (1.468 Å).[15b] This finding can be related to the fact that the positive charge is delocalized in the Zn complex-catalyzed process, compared with a more localized charge on H_3O^+.

Assisted Mechanism (TS2C). A transition state corresponding, as above, to the nucleophilic attack of the carbonyl group by an oxygen atom of the water dimer has been located. The activation energy, calculated with respect to the catalyzed formamide and two free water molecules, remains rather high (+36.27 kcal/mol, Table 3) but exhibits a lower value than the one found in the previous mechanism. Considering the geometrical parameters (Table 1, and Figure 2b for the structure), note that the ZnO_1 bond is shorter than that in TS1C (by 0.026 Å) and leads to a longer C_1O_1 bond and a shorter C_1N_1 bond. However, C_1N_1 remains longer than the one computed in FoC. In conjunction, the C_1O_1' bond length (1.488 Å) decreases with respect to TS1C, while the proton transfer between the water dimer and the nitrogen atom of formamide is delayed (N_1H_2, 1.765 Å). Here, assistance by an ancillary water molecule increases the nucleophilicity of the attacking water molecule.[46] As discussed elsewhere,[15] a second transition state, corresponding to the breaking of the CN bond, should occur in the potential energy surface, but it is expected to present a lower energy barrier. Therefore, this stationary point has not been considered here.

Again, compared with the case of the nonassisted reaction, the charge transfer from the reactive part to the catalyst (+0.316 e) has increased. The charge of formamide is now −0.231 e, while that of the water dimer is +0.547 e. The electronic transfer occurs essentially from the water molecules to formamide and then to the catalyst. Among the atoms of the water dimer, the H-bonded accepting oxygen atom is the main electron-donating atom. The charge of the metal changes only slightly (−0.011 and −0.004 e compared to FoC and TS1C, respectively). The most important part of the charge is delocalized on the ligands, especially on the formate group.

IV. Enzymatic Reaction: Mechanisms Involving the Whole Thermolysin Molecule

A. Definition of the Quantum and Classical Parts: Optimization with Water. The optimized structure presented above has been divided in two subsystems: the first will be described quantically (QS), and the second will be described classically (CS) (see Chart 1). In the former, the metal cation Zn^{2+}, the side chains of the ligands (the Cα atom is the frontier atom between the two subsystems), and the fourth ligand of the zinc atom (i.e., water molecule or formamide) are included. Further, the water molecules involved in the hydrolysis mechanisms will be part of the quantum subsystems. The classical subsystem corresponds to the rest of the enzyme and water molecules.

In CS, the atoms have been kept fixed during the optimizations of the quantum part, while in QS only the frontier atoms and the internal coordinates which include these frontier atoms are fixed during the optimizations. By comparison with the model of active site considered above, one additional CH_2 group replaces one hydrogen atom on each ligand in the QS. In addition, the presence of the enzyme allows us to relax the structure of the catalytic center.

The resulting structure is close to the optimized classical geometry. The main difference is observed in the position of the water molecule, which constitutes the fourth ligand of the zinc atom due to the interactions with the surrounding amino acids. One of the hydrogen atoms of the water molecule interacts with an oxygen atom of the carboxylic group of Glu143 (2.25 Å). There is also an interaction between the oxygen atom of the water molecule and a hydrogen atom of $His231^+$ (2.56 Å). Even though these distances are long, they are important to understanding the configuration of the water molecule, which is rather different from those previously obtained with the model of active site. This situation is easy to understand, owing to the large electrostatic contribution to the interaction energy of the reacting species with their surroundings.

B. Formamide−Thermolysin Complex (FoT). In this complex, the water molecule interacting with the zinc atom has been replaced by the formamide molecule. After optimization of the quantum part, the geometries of the ligands are only slightly modified (see Figure 3). The configuration of the formamide is different from that found in the previous study.

(46) Bertrán, J.; Ruiz- López, M. F.; Rinaldi, D.; Rivail, J.-L. *Theor. Chim. Acta* **1992**, *84*, 181 and references therein.

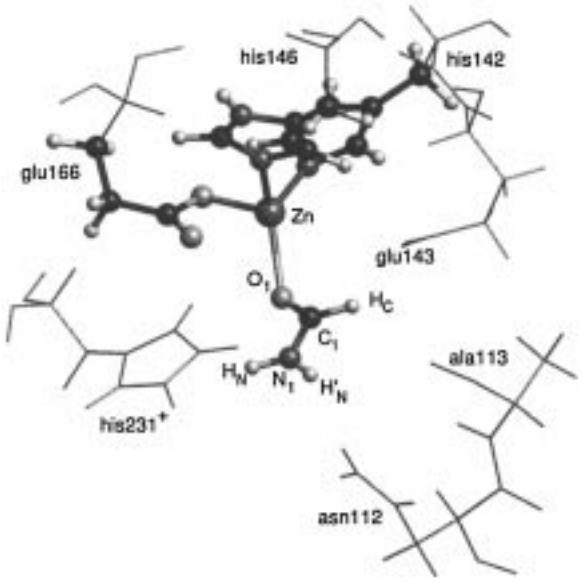

Figure 3. Formamide−thermolysin complex, FoT. The quantum part is represented in balls and sticks, while the closest amino acids of the classical part are represented by lines.

The steric hindrance is certainly not the only explanation, since the cavity shape near the active site is large enough for the formamide molecule to rotate around the ZnO_1 bond. Interactions with the surrounding amino acids have to be taken into account again to explain the position of the formamide. First, it can be noted that H_C and the oxygen atoms of the Glu143 carboxylic group are close (2.29 and 2.66 Å, see Figure 3). On the opposite side, the distance between O_1 and a hydrogen atom of His231$^+$ is 2.42 Å.

C. Hydrolysis Reaction Study. The reaction paths for both nonassisted and water-assisted hydrolysis mechanisms are presented in Scheme 1. These mechanisms are more complex than the two previous cases: both mechanisms exhibit an intermediate state. Owing to the importance of this system, the second transition state has been characterized in both mechanisms. Concerning the nonassisted mechanism, the initial complex is denoted I1, and the first transition state, corresponding to the nucleophilic attack by the oxygen atom of the water molecule, is denoted TS1T. The intermediate species is I1′, the second transition state, which corresponds to the total breaking of the C_1N_1 bond is TS1′, and the products are denoted P1. For the assisted mechanism, the respective stationary points are denoted I2, TS2T, I2′, TS2′, and P2.

Nonassisted Mechanism. The TS1T structure is presented in Figure 4a, geometrical parameters and Mulliken net atomic charges are compiled in Table 4, and the energies (and energy variations) are shown in Table 6 and in Figure 5.

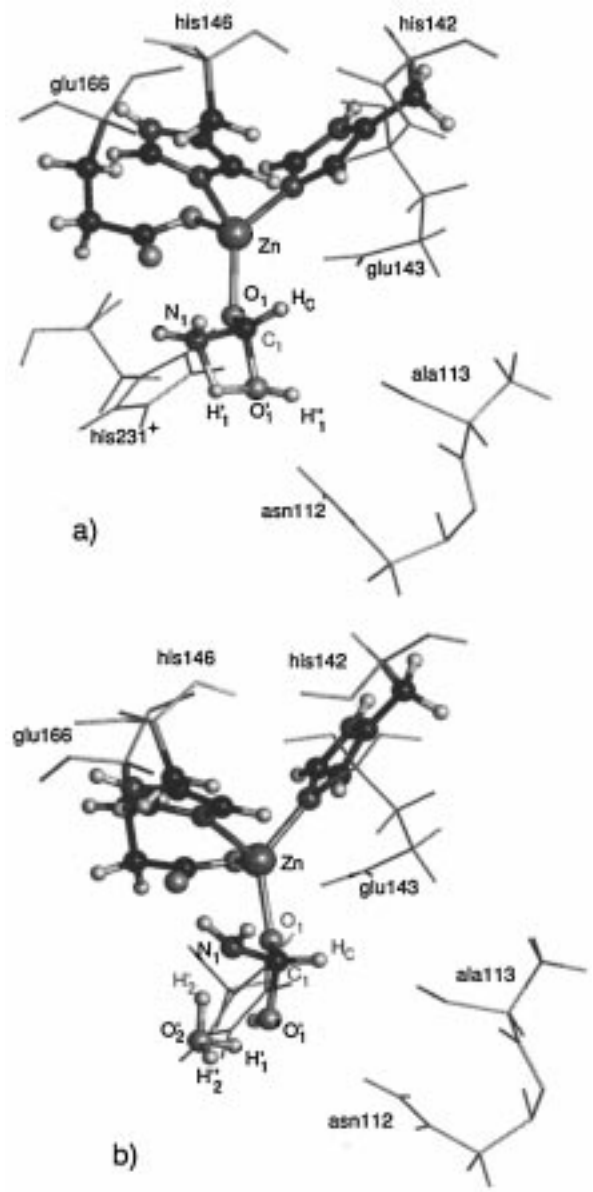

Figure 4. Transition states for the reactions catalyzed by thermolysin, (a) for the nonassisted and (b) for the water-assisted mechanisms (denoted TS1T and TS2T, respectively). The quantum part is represented in balls and sticks, while the closest amino acids of the classical part are represented by lines.

(a) Initial Complex I1. The incoming water molecule is still far from the formamide molecule ($O_1'C_1$, 5.359 Å) and is mainly interacting with the surrounding amino acids. Thus,

Scheme 1

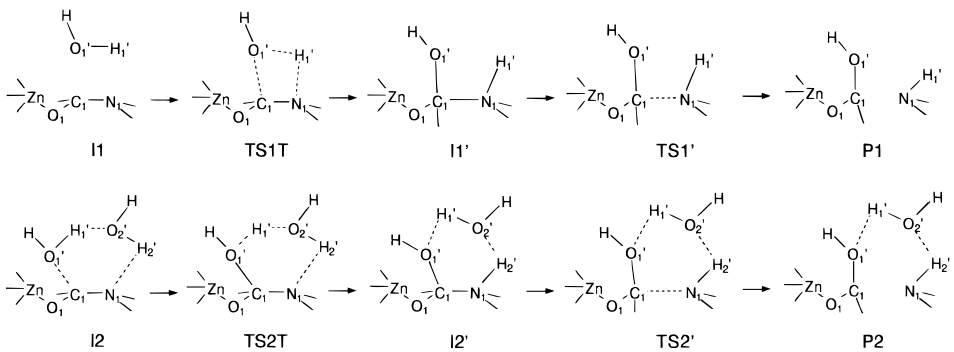

Table 4. Geometrical Parameters (Distances in Anstroms, Angles in Degrees) and Mulliken Net Atomic Charges for the Complex Formamide−Thermolysin and the Stationary Points of the Nonassisted Formamide Hydrolysis Mechanism Catalyzed by Thermolysin[a]

	FoT	I1	TS1T	I1′	TS1′	P1
Geometrical Parameters						
ZnO1	2.225	2.227	2.154	2.136	2.168	2.203
C_1O_1	1.278	1.278	1.305	1.312	1.284	1.252
C_1N_1	1.352	1.352	1.503	1.628	1.862	3.371
C_1O_1'		5.359	1.550	1.416	1.393	1.354
$O_1'H_1'$		0.962	1.264	2.681	2.836	3.974
$H_1'N_1$		5.233	1.381	1.010	1.001	0.998
$H_1'O_1'C_1N_1$		287.03	357.31	336.78	338.57	347.91
$ZnO_1C_1N_1$	87.02	87.04	99.74	57.82	62.45	45.45
Mulliken Population Analysis						
His 142	0.397	0.397	0.388	0.387	0.390	0.400
His146	0.295	0.295	0.276	0.257	0.276	0.306
Glu166	−0.547	−0.546	−0.569	−0.559	−0.554	−0.546
Zn	0.740	0.740	0.734	0.729	0.739	0.731
reactive part	0.201	0.200	0.258	0.272	0.234	0.194
Fo	0.201	0.200	0.023			
H_2O		0.000	0.235			
NH_3				0.460	0.270	0.000
HCOOH				−0.188	−0.036	0.193

[a] See text and Figure 4a for notations.

Table 5. Geometrical Parameters (Distances in Angstroms, Angles in Degrees) and Mulliken Net Atomic Charges for the Stationary Points of the Water-Assisted Formamide Hydrolysis Mechanism Catalyzed by Thermolysin[a]

	I2	TS2T	I2′	TS2′	P2
Geometrical Parameters					
ZnO1	2.209	2.119	2.129	2.167	2.194
C_1O_1	1.278	1.331	1.319	1.282	1.260
C_1N_1	1.368	1.482	1.611	1.948	2.313
C_1O_1'	2.288	1.522	1.415	1.381	1.363
$O_1'H_1'$	0.962	1.326	2.130	2.161	2.177
$H_1'O_2'$	2.240	1.129	0.967	0.964	0.964
$O_2'H_2'$	0.961	1.098	2.122	2.177	2.197
$H_2'N_1$	3.998	1.543	1.017	1.003	1.001
$ZnO_1C_1N_1$	73.34	51.73	52.64	79.98	80.13
$H_2'N_1C_1O_1'$	11.21	5.72	5.99	7.74	7.97
Mulliken Population Analysis					
His 142	0.391	0.380	0.381	0.383	0.393
His146	0.296	0.264	0.275	0.292	0.306
Glu166	−0.563	−0.585	−0.572	−0.566	−0.559
Zn	0.743	0.736	0.739	0.746	0.749
reactive part	0.206	0.291	0.261	0.225	0.197
Fo	0.189				
$[H_2O]_2$	0.017/0.000				
NH_3		−0.275[b]	0.460	0.234	0.062
H_2O		0.556[c]	0.009	0.019	0.034
HCOOH			−0.208	−0.028	0.101

[a] See text and Figure 4b for notations. [b] Sum of the net atomic charges of the atoms of the reactive part except O_2', H_1', H_2', H_2''. [c] Charge of the $[H_3O^+]$-like entity: O_2', H_1', H_2', and H_2'' atoms.

geometrical parameters and charge distribution of the quantum part do not change with respect to the FoT complex.

(b) Transition State TS1T. This structure presents the same trends as the one found in TS1C. Here again, the perturbation of the formamide p-system leads to an increase of the C_1O_1 (+0.027 Å) and C_1N_1 (+0.151 Å) bonds with respect to FoT. The O_1' oxygen approach on the C_1 atom is favored compared to the H_1' hydrogen approach on N_1 (C_1O_1', 1.550 Å, and $H_1'N_1$, 1.381 Å). The charge transfer (+0.258 e) from the reactive part to the metal and its ligands comes essentially from the water molecule (0.235 vs 0.023 e for the formamide) and is distributed over the ligands (see Table 4). Some strong interactions between quantum and classical atoms can be reported: H_C with the carboxylic oxygen atoms of Glu143 (2.27 and 2.21 Å); O_1 and O_1' with the His231+ hydrogen atom (2.23 and 2.32 Å, respectively); H_1' with the Ala113 carbonyl oxygen (2.23 Å).

Table 6. Contributions of the Total Energy for the Stationary Points[a] of the Hydrolysis Reactions Mechanisms: EC_{elec}, EC_{vdW}, and EC_{Total}, in kcal/mol

Nonassisted Mechanism					
	I1	TS1T	I1′	TS1′	P1
EC_{elec}	−242.13	−237.30	−246.24	−243.69	−246.21
EC_{vdW}	6.40	6.53	6.65	6.54	6.17
EC_{total}	−235.74	−230.77	−239.59	−237.15	−240.04
Water-Assisted Mechanism					
	I2	TS2T	I2′	TS2′	P2
EC_{elec}	−240.48	−233.72	−241.81	−240.61	−238.78
EC_{vdW}	6.25	5.88	5.66	5.26	5.18
EC_{total}	−234.24	−227.84	−236.15	−235.35	−233.60

[a] The values for the formamide−thermolysin complex are EC_{elec} = −239.94 kcal/mol, EC_{vdW} = 8.06 kcal/mol, and EC_{Total} = −231.89 kcal/mol.

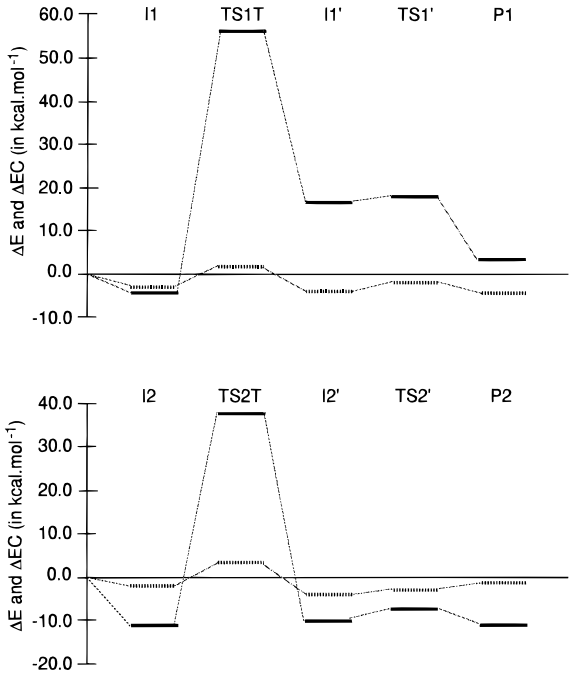

Figure 5. Potential energy surfaces for the nonassisted and the water-assisted mechanisms. Relative energies ΔE are shown in plain lines, and relative energy contributions of the enzyme ΔEC are shown in hatched lines.

(c) Intermediate I1′. The C_1N_1 bond is not completely broken (1.628 Å), though the NH_3 group is almost formed. This strong interaction with the formate moiety is visible if one analyzes the charge transfer: the NH_3 group gives 0.460 e to the rest of the system. This charge is mainly located on the formate group, but a small part is transferred to the catalytic center (see Table 4). The distance between H1′ and the Ala113 carbonyl oxygen is now 2.93 Å.

(d) Transition State TS1′. It corresponds to the cleavage of the amidic bond. C_1N_1 is almost broken: 1.862 Å. There is still an important electron transfer to the catalyst (0.244 e), but one notices that the NH_3 moiety gives 0.270 e to the rest of the system. Several interactions with the surrounding amino acids are weakened, and the HCOOH group is not far from planarity ($O_1C_1O_1'H_C$, 35.6°).

(e) Products P1. In the last stationary structure, C_1N_1 is broken (3.371 Å), and one formic acid molecule and one ammonia molecule are clearly identified. There is still a charge transfer to the catalytic center which comes, now, from the formic acid molecule only. The net charge of the Zn atom remains almost constant. Therefore, the fact that the ligands act as an electron reservoir is confirmed.

Water-Assisted Mechanism. The corresponding data are presented in Figure 4b for the structure and notations, in Table 5 for the geometrical parameters, and in Table 6 and Figure 5 for the energies.

(a) Initial Complex I2. As expected considering previous results,[15a] this complex consists of a weakly bonded complex between formamide and the water dimer. This complex presents a partially formed C_1O_1' bond (2.288 Å), while no N_1H_2' weak bond is predicted (N_1H_2', 4.998 Å). Nevertheless, pyramidalization of the nitrogen atom has occurred ($H_NN_1H_N'C_1$, 30.59°). The ZnO_1 bond changes only slightly with respect to FoT (2.209 vs 2.225 Å, respectively).

(b) Transition State TS2T. The transition state presents the same general trends as those found in TS2C. As expected, C_1O_1 and C_1N_1 increase with respect to FoT (+0.055 and +0.130 Å, respectively). The nucleophilic approach of the water molecule is favored over the electrophilic one (C_1O_1', 1.522 Å, and N_1H_2', 1.543 Å) and a $[H_3O]^+$-like entity can be recognized, involving the H_1', O_2', and H_2' atoms and the second hydrogen atom of the O_1' oxygen atom. Nevertheless, the structure of the six-membered ring is not far from planarity (5.72° deviation only). If one considers the configuration at the nucleophilic oxygen atom, one notices a strong difference with the case of the nonassisted mechanism. The H-bonded hydrogen atom being denoted H_1'', the $O_1C_1O_1'H_1''$ dihedral angle is close to 180° in the TS1T structure and close to 0° in the TS2T one. This configuration, in particular the planarity of the six-membered ring, appears to be a consequence of the interaction with the neighboring side chains. In particular, the interactions of the amino group and the carboxylic group of Glu143 are stronger than those in TS1T (the hydrogen−oxygen distance is decreased from 2.72 to 2.23 Å in TS2T). Like in the previous water-assisted mechanism, the charge transfer going from the reactive part to the catalyst is more important than that in the nonassisted mechanism (0.291 vs 0.258 e).

(c) Intermediate I2′. In this intermediate, though the hydrolysis process has occurred (N_1H_2', 1.017 Å, and C_1O_1', 1.415 Å), a weak amidic bond still exists (C_1N_1, 1.611 Å). The water molecule formed by the H_1' and O_2' atoms and the second hydrogen atom of the O_2' oxygen atom solvates the structure and stabilizes the CN bond with respect to the one obtained in TS1T (C_1N_1, 1.628 Å). The six-membered ring remains close to planarity in this structure ($H_2'N_1C_1O_2'$, 5.99°).

Transition State TS2′. This transition state corresponds to the breaking of the C_1N_1 bond. Again, a relatively important electron transfer exists, going from the NH_3 group to the HCOOH one (0.270 e), even if the C_1N_1 distance is long (1.948 Å).

(e) Products P2. In this structure, HCOOH and NH_3 molecules are well characterized but remain close due to stabilization by the second water molecule.

V. Discussion

In the mechanisms involving the whole enzyme, the first transition states (TS1T and TS2T), which correspond to the insertion of the water molecules, are the rate-limiting step of the reactions. The activation energies are tabulated in Table 3, together with the corresponding quantities for the molecular processes. They are higher than those previously computed with the simple model of the active site (TS2C and TS1C). If this increase in energy is relatively large for the nonassisted process (almost +6 kcal/mol), it remains rather small in the case of the water-assisted mechanism (about +2 kcal/mol). These differences result from changes in the activation of the formamide molecule. Since the catalysts are very similar, it is clear that the surrounding amino acids play an important role on this activation. First, the charge transfer from formamide to thermolysin (+0.201 e) is less important than the charge transfer to the model catalyst (+0.334 e), and the bond between the O_1 oxygen atom and the metal is longer in the former case. However, the charge of the zinc atom is only slightly modified (+0.740 vs +0.756 e, respectively); the most important delocalization is supported by the ligands. These differences, as mentioned above, arise from the position of the formamide molecule in the cavity shape and are directly related to interactions with some amino acids described classically. This slightly distorted configuration obviously contributes to the higher activation energy, which means a less efficient activation of the peptidic bond in the enzyme. Nevertheless, one should keep in mind that the geometry of the active center is optimized in the case of the enzymatic reaction, although the ligands of the zinc ions, other than the reactants, are kept fixed in the case of the model catalyst. This means that the energy barriers found in this case can be considered as lower bounds of the predicted activation energy in the actual case simulated by this model catalyst. Therefore, the agreement between the computed energies in both systems is probably better than it looks.

If one compares the activation energies computed in both the complex-catalyzed and the enzyme-catalyzed reactions to the corresponding quantities computed for the proton-catalyzed mechanisms and the neutral ones, one notices that both the complex and the enzyme give rise to an intermediate activation barrier between the latter cases. This can be directly related to the moderate Lewis acidity of the catalyst.

In every system considered here or in a previous study in aqueous solution, a general finding is that all the catalyzed processes start with a nucleophilic attack on the carbonyl group, either for the nonassisted mechanisms or the assisted ones. The differences in the values of the activation energies are reproduced in the differences of the C_1O_1' carbon−oxygen distance. We already mentioned, in the case of the enzyme, the role of the interactions with the rest of the protein, which is absent in the case of the protein-free complex. For each type of process (nonassisted and water-assisted), the increase of the C_1O_1' bond length is balanced by a decrease of the N_1H_2' bond length. The water-assisted processes are more favorable, due to the larger nucleophilicity of the oxygen atom in the water dimer and the formation of a six-membered ring in the first transition state. Another difference between these two processes is that the second proton of the attacking water molecule is directly transferred to the nitrogen atom in the nonassisted process, although it is transferred to the second water molecule in the water-assisted ones, giving rise to a H_3O^+ ion and also a two-step reaction. The difference between these two processes is almost negligible in the neutral reaction and increases as the strength of the acid catalyst increases.

The influence of the enzyme on the reaction processes can be analyzed in more detail. Table 6 and Figure 5 illustrate the various contributions to the interaction energy between the quantum and the classical subsystems. These contributions are respectively the electrostatic interaction, EC_{elec}, the van der

Waals one, EC_{vdW}, and their sum, EC_{total}. The important electrostatic interaction is, for a large part, explained by the fact that the quantum subsystem is positively charged, and the rest of the enzyme is negatively charged. More interesting are the variations of these quantities. The stabilizing contributions of the enzyme−substrate interaction are clear (see Table 6). These interactions introduce a constraint on the transition-state geometries which slightly increases the first energy barrier (see Figure 5). These quantities are in qualitative agreement with results obtained in the case of the water-assisted proton-catalyzed reaction, in which the enzyme has been modeled by a continuum[15a] with a dielectric constant of 2, in which the barrier is increased by 1−2 kcal mol^{-1}. The surrounding protein plays another important role in stabilizing the intermediate structures I1′ and I2′ and destabilizing the transition states so that, in the nonassisted process, a second transition state occurs such as in the water-assisted one.

Finally, the overestimation of the energy barriers induced by the use of the semiempirical AM1 method can be estimated by comparing the computed values with the results of single-point computations performed on the stationary point geometries at the BLYP DFT level in the case of the complex catalyst. The TS1C barrier is reduced from 50.0 to 39.9 kcal mol^{-1} in the nonassisted mechanism and the TS2C barrier from 36.3 to 18.5 kcal mol^{-1} in the water-assisted one.

Conclusion

The study of the hydrolysis of a formamide molecule catalyzed both by a model of the thermolysin active site and the whole enzyme confirms a decrease of the activation barriers when a second water molecule is introduced in the reaction coordinate (bifunctional catalysis), as found in the case of the acid catalysis. Additionally, the preferential nucleophilic approach of the reacting water molecules on the carbon atom involved in the amidic bond of formamide, considered as a model of a peptidic bond, is clearly shown in both water-assisted and nonassisted mechanisms.

The analyses of the mechanisms catalyzed by a model of the thermolysin active site or by the whole protein show that the catalytic effect is moderate due to a medium Lewis acidity of the zinc complex but prove the role as an electron reservoir of the metal ligands along the reaction paths. The macromolecular structure of the enzyme is expected to slightly increase the energy barriers, due to a distortion of the structures occurring along the reaction path, but this increase is very small and of the order of magnitude of the error bars on energy values. In contrast, a crucial role is expected from the macromolecular surroundings of the reaction center: the recognition of the part of the substrate to be hydrolyzed. In addition, the stability of the enzyme−substrate complex is expected to greatly increase the probability of the reaction to take place. These aspects, which obviously play an important role in the selectivity and the regulation of the biological processes in which thermolysin is involved, will be addressed in a forthcoming study.[29]

Acknowledgment. The authors thank Prof. B. P. Roques (U266 INSERM, URA D1500 CNRS), his group working on metalloproteases, and Dr. B. Maigret for fruitful discussions. We acknowledge the support of the Centre Charles Hermite in Nancy for the provision of computer time on the SG Power Challenge machines and for the kind help of their technical staff.

JA981650U